International Immunology, Vol. 31, No. 12, pp. 781–793
doi:10.1093/intimm/dxz048
Advance Access publication 14 June 2019

Metabolic adaptation to glycolysis is a basic defense mechanism of macrophages for *Mycobacterium tuberculosis* infection

Mayuko Osada-Oka[1], Nobuhito Goda[2], Hiroyuki Saiga[3,9], Masahiro Yamamoto[3,10,11], Kiyoshi Takeda[3], Yuriko Ozeki[4], Takehiro Yamaguchi[4,12], Tomoyoshi Soga[5], Yu Tateishi[6], Katsuyuki Miura[6], Daisuke Okuzaki[7], Kazuo Kobayashi[8] and **Sohkichi Matsumoto[4]**

[1]Food Hygiene and Environmental Health, Graduate School of Life and Environmental Science, Kyoto Prefectural University, Kyoto, Kyoto 606-8522, Japan
[2]Department of Life Science and Medical BioScience, Waseda University School of Advanced Science and Engineering, Shinjuku-ku, Tokyo 162-8480, Japan
[3]Department of Microbiology and Immunology, Graduate School of Medicine, Osaka University, Suita, Osaka 565-0871, Japan
[4]Department of Bacteriology, Niigata University Graduate School of Medical and Dental Sciences, Niigata, Niigata 951-8510, Japan
[5]Institute for Advanced Biosciences, Keio University, Tsuruoka, Yamagata 997-0052, Japan
[6]Department of Applied Pharmacology and Therapeutics, Osaka City University Graduate School of Medicine, Osaka, Osaka 545-8585, Japan
[7]Genome Information Research Center, Research Institute for Microbial Diseases, Osaka University, Suita, Osaka 565-0871, Japan
[8]Division of Public Health, Osaka Institute of Public Health, Osaka, Osaka 537-0025, Japan
[9]Present address: Department of Immunology Faculty of Medicine, Kagawa University, Kida-gun, Kagawa 761-0793, Japan
[10]Present address: Department of Immunoparasitology, Research Institute for Microbial Diseases, Osaka University, Suita, Osaka 565-0871, Japan
[11]Present address: Laboratory of Immunoparasitology, WPI Immunology Frontier Research Center, Osaka University, Suita, Osaka 565-0871, Japan
[12]Present address: Department of Pharmacology, Osaka City University Graduate School of Medicine, Osaka, Osaka 545-8585, Japan

Correspondence to: M. Osada-Oka; mayuko-oka@kpu.ac.jp

Received 12 November 2018, *editorial decision* 10 June 2019; *accepted* 26 June 2019

Abstract

Macrophages are major components of tuberculosis (TB) granulomas and are responsible for host defenses against the intracellular pathogen, *Mycobacterium tuberculosis*. We herein showed the strong expression of hypoxia-inducible factor-1α (HIF-1α) in TB granulomas and more rapid death of HIF-1α-conditional knockout mice than wild-type (WT) mice after *M. tuberculosis* infection. Although interferon-γ (IFN-γ) is a critical host-protective cytokine against intracellular pathogens, HIF-1-deficient macrophages permitted *M. tuberculosis* growth even after activation with IFN-γ. These results prompted us to investigate the role of HIF-1α in host defenses against infection. We found that the expression of lactate dehydrogenase-A (LDH-A) was controlled by HIF-1α in *M. tuberculosis*-infected macrophages IFN-γ independently. LDH-A is an enzyme that converts pyruvate to lactate and we found that the intracellular level of pyruvate in HIF-1α-deficient bone marrow-derived macrophages (BMDMs) was significantly higher than in WT BMDMs. Intracellular bacillus replication was enhanced by an increase in intracellular pyruvate concentrations, which were decreased by LDH-A. Mycobacteria in phagosomes took up exogenous pyruvate more efficiently than glucose, and used it as the feasible carbon source for intracellular growth. These results demonstrate that HIF-1α prevents the hijacking of pyruvate in macrophages, making it a fundamental host-protective mechanism against *M. tuberculosis*.

Keywords: granuloma, hypoxia-inducible factor-1α, pyruvate, tuberculosis

Introduction

Mycobacterium tuberculosis is the causative agent of tuberculosis (TB), one of the three most serious infectious diseases, which killed 1.8 million individuals in 2016. *Mycobacterium tuberculosis* is a typical intracellular bacterium, and even after being engulfed by a macrophage, it may replicate within cells. Macrophages and their activation by interferon-γ (IFN-γ) are known to be primarily responsible for host protection against *M. tuberculosis* and other intracellular pathogens (1). IFN-γ is a cytokine that is mainly produced by T lymphocytes, and activates the bactericidal and bacteriostatic functions of macrophages.

Hypoxia-inducible factor-1 (HIF-1) is a transcriptional regulator of host cells. It is a heterodimer composed of HIF-1α and HIF-1β (2, 3). HIF-1α is virtually undetectable under normoxic conditions because it is degraded by proteasomes, whereas HIF-1β is constitutively expressed in cells (4, 5). These findings indicate that HIF-1α is a key factor controlling the functions of HIF-1 and hypoxic responses of cells. Schaible *et al*. demonstrated that hypoxia markedly attenuated the internalization of the human opportunistic pathogen *Pseudomonas aeruginosa* into epithelial cells (6). In addition to its role in hypoxic responses, HIF-1 has been shown to contribute to defenses against pathogen infections. Mice lacking HIF-1α in their myeloid cell lineage exhibited decreased bactericidal activity and failed to restrict the systemic spread of infection from an initial tissue focus (7). HIF-1 controls the production of inducible nitric oxide synthase (iNOS), an antimicrobial enzyme. A recent study demonstrated that HIF-1 was critical for the control of *M. tuberculosis* through the activation of IFN-γ-dependent bactericidal mechanisms, such as the production of iNOS, interleukin and prostaglandin by macrophages (8). However, the functions of HIF-1 and IFN-γ cannot completely overlap. There may be a remaining unknown HIF-1-specific function in host protection against *M. tuberculosis* infection.

In the present study, we examined the IFN-γ-independent host-protective contribution of HIF-1 in *M. tuberculosis*-infected macrophages. The results showed that lactate dehydrogenase-A (LDH-A) was induced in *M. tuberculosis*-infected macrophages by HIF-1, but not by IFN-γ. LDH-A mediates glucose metabolism by converting lactate to pyruvate. We herein demonstrated that the HIF-1-dependent up-regulation of LDH-A is a fundamental host-protective mechanism of macrophages against *M. tuberculosis* infection.

Methods

Materials

EnVision™ kits, horseradish-peroxidase (HRP)-conjugated goat anti-mouse immunoglobulin G (IgG) and goat anti-rabbit IgG were obtained from Dako/Agilent (Santa Clara, CA, USA). A polyclonal anti-HIF-1α antibody was from Cayman (Ann Arbor, MI, USA). Anti-HIF-2 and anti-HIF-1β antibodies were obtained from Novus Biologicals (Litteton, CO, USA), and anti-LDH-A antibody was from Proteintech (Rosemont, IL, USA). Dulbecco's modified Eagle's medium (DMEM) with pyruvate and IFN-γ were obtained from Wako Pure Chemical Industries Ltd (Osaka, Japan) and DMEM without pyruvate was obtained from Nacalai Tesque (Kyoto, Japan). Fetal bovine serum (FBS) was from Equitech Bio (Kerrville, TX, USA). An anti-β-actin antibody and oxamate were purchased from Sigma (St Louis, MO, USA). Isogen was obtained from Nippon Gene (Toyama, Japan) and the ReverTra Ace qPCR RT Kit was from Toyobo (Osaka, Japan). The Ambion PARIS™ Kit and TaqMan gene expression master mix were purchased from Applied Biosystems (Carlsbad, CA, USA). SYBR Green real-time PCR master mix was purchased from Roche/Nippon Genetics (Tokyo, Japan). [^{14}C]-Pyruvate was obtained from the Japan Radioisotope Association (Tokyo, Japan).

Histopathology and immunohistochemistry

To infect BALB/c (or C57BL/6) mice (n = 7 or 3) with *M. tuberculosis* Erdman or H37Rv, the nebulizer of the Middlebrook airborne infection apparatus (Glas-Col, Terre Haute, IN, USA) was filled with 5-ml phosphate-buffered saline containing 5×10^6 colony-forming units (CFU) of bacteria, and mice were exposed for 90 min using the Glas-Col aerosol generator. This procedure deposits ~10 CFU of bacteria into the lungs. These mice were euthanized 3–5 weeks after infection. The lungs were harvested, fixed in 10% formaldehyde and then embedded in paraffin. Lung sections were stained with hematoxylin–eosin to visualize tissue morphology and also with Ziehl–Neelsen staining. Specimens were immunohistochemically stained with the Dako EnVision™ system, according to the manufacturer's instructions, with a polyclonal anti-HIF-1α antibody (1:200) provided by Sang-You Ye (Soul National University), and with an anti-mycobacterial DNA-binding protein 1 (MDP1) antibody raised in a rabbit (1:500). All mice were maintained under specific pathogen-free conditions in a biosafety level-3 facility at the Research Institute of Tuberculosis according to the standard guidelines for animal experiments with the approval of their Ethical Committees.

Mice

HIF-1α$^{fl/fl}$ mice were crossed with mice expressing Cre recombinase under the control of the lysozyme M promoter (LyzM-Cre$^{+/+}$ mice; Jackson Laboratories, Bar Harbor, ME, USA). The offspring of this mating were HIF-1α$^{fl/fl}$-LyzM-Cre$^{+/-}$ [i.e. HIF-1α deletable; HIF-1α conditional knockout in their myeloid cell lineage (HIF-1 CKO)] or HIF-1α$^{fl/fl}$-LyzM-Cre$^{-/-}$ [i.e. HIF-1α-non-deletable littermate controls; wild-type (WT)]. PCR on mouse genomic DNA was used to detect the floxed HIF-1α gene and Cre transgene with appropriate primers (Supplementary Table 1). iNOS knockout mice were a gift from Dr Yasukatsu Izumi (Osaka City University, Japan). Toll-like receptor 2 (TLR2), TLR4 and TLR9 knockout mice were from Oriental Bio Service (Kyoto, Japan). All mice were maintained under specific pathogen-free conditions in the animal facilities of Osaka City University Graduate School of Medicine, Kyoto Prefectural University and in a biosafety level-3 facility at Niigata University according to the standard guidelines for animal experiments at each institute with the approval of their Ethical Committees.

Estimation of mouse survival after infection with M. tuberculosis

WT and HIF-1 CKO mice (n = 12 and 11) were infected with 2×10^6 CFU of *M. tuberculosis* strain H37Rv via the intra-tracheal

route. Survival data were analyzed by the construction of Kaplan–Meier plots and with Log-rank analyses (Mantel–Cox test). All mice were maintained under specific pathogen-free conditions in a biosafety level-3 facility at Osaka University according to the standard guidelines for animal experiments with the approval of their Ethical Committees.

Construction of kanamycin-resistant Mtb-luc and BCG-luc

The plasmid expressing firefly luciferase was constructed previously (9) and introduced into *M. tuberculosis* H37Rv by electroporation as described previously (10), and the kanamycin-resistant *M. tuberculosis*-luciferase (rMtb-luc) strain was obtained. rMtb-luc and the kanamycin-resistant *M. bovis* bacillus Calmette–Guerin (BCG)-luciferase (rBCG-luc) strain (9) were cultured in 7H9-ADC media containing 10 μg ml^{-1} kanamycin at 37°C until the mid-logarithmic phase.

Cell culture

Bone marrow was flushed from the femur and tibia of mice, and cells were plated in dishes with DMEM containing 10% FBS, 4.5 g l^{-1} glucose and 20% conditioned medium from the supernatants of macrophage colony-stimulating-factor-secreting L929 (LC14) fibroblasts. Bone marrow cells differentiated into macrophages in 7–10 days and were then used in experiments. To examine the intracellular growth of *M. tuberculosis*, mouse bone marrow-derived macrophages (BMDMs) (5×10^4 cells per well) seeded on 96-well plates were infected with rMtb-luc [multiplicity of infection (MOI) = 0.5] or rBCG-luc (MOI = 2.0) for 12 h in DMEM excluding FBS, and extracellular bacilli were removed from the macrophage culture medium. In western blotting, real-time PCR and microarrays, *M. tuberculosis* H37Rv (MOI = 0.5) or *M. bovis* BCG (MOI = 2.0), excluding the plasmid expressing luciferase, were infected for 12 h in mouse BMDMs (2×10^6 cells per well) seeded on six-well plates. After extracellular bacilli had been removed from the macrophage culture medium, cells were cultured for 24 h or 4 days in the absence or presence of 500 U ml^{-1} IFN-γ. Whole-cell lysates were used for immunoblotting or gene expression analyses.

Ldh-A-deleted RAW264.7 cells

For deletion of *Ldh-A* in RAW 264.7 cells, we applied CRISPR/Cas9 genome editing. We used CRISPR DIRECT (http://crispr.dbcls.jp) to minimized off-target effects, and single-guide RNA (sgRNA) was designed for targeting exon4 of mouse *Ldh-A* (3′-CGGGGGCCCGTCAGCAA GAG-5′). After annealing with forward oligo (5′-CACCG CGGGGGCCCGTCAGCAAGAG-3′) and reverse oligo (5′-AAAC CTCTTGCTGACGGGCCCCCG C-3′) at 92, 72, 55 and 37°C for each of 2 min, oligo duplex was ligated with hSpCas9(BB)-2A-Puro (PX459) V2.0 (Addgene, Cambridge, MA, USA), which was digested with *Bbs*I endonuclease using T4 ligase at 37°C for 10 min. RAW264.7 cells (2×10^4 cells per well) were spread in six-well plates and cultured for 24 h at 37°C. Cells were transfected with PX459-m*LdhA* plasmid (1 μg) using Lipofectamine3000 (2.5 μl) and p3000 reagent (2 μl) in Opti-MEM (0.5 ml per well). After incubation for 24 h, cells were selected by puromycin (6 μg ml^{-1}) for 24 h. Clonal cells were collected and confirmed deletion of *Ldh-A* mRNA by real-time PCR and a decrease in LDH-A expression by western blotting.

Immunoblotting analysis

The immunoblotting analysis was performed with antibodies directed against HIF-1α (C-term) (1:500) (Cayman), HIF-2α (1:500), HIF-1β (1:1000), iNOS (1:1000), LDH-A (1:1000) and β-actin (1:5000). Blotted proteins were visualized with HRP-conjugated goat anti-rabbit IgG or goat anti-mouse IgG antibody and Immobilon Western Chemiluminescent HRP substrate (Merck/Millipore, Tokyo, Japan). The amount of protein detected by some antibodies was measured using a computed image analysis system (Image Quant LAS-4000 mini, GE Healthcare UK, Buckinghamshire, UK). The viewing of digitized images were performed using Image Quant LAS-4000 mini Control Software and Image J.

Isolation of total RNA and real-time PCR

Total RNA (1 μg) extracted from macrophages using the PARIS™ Kit or Isogen, according to the manufacturer's instructions, was transcribed into cDNA with the ReverTra Ace® qPCR RT Kit in a total volume of 10 μl, according to the manufacturer's instructions. cDNAs were then used as templates for PCR amplification using the TaqMan probe Master Mix or SYBR Green PCR Master Mix using the ABI 7900HT Fast Real-Time PCR System (Applied Biosystems, Foster City, CA, USA). We used the TaqMan probe assay for *Hif-1α*, *Ldh-A* and 18S rRNA (Supplementary Table2). In analyses of *iNos* and *Irgm*, we used SYBR Green (Roche). The interpolated values for each sample were divided by the corresponding values for 18S rRNA, as the housekeeping gene, and the results obtained were expressed as the ratio of relative intensity for a specific gene/18S rRNA. Real-time PCR reactions were performed at 95°C for 10 min, followed by 40 cycles at 95°C for 15 s and at 60°C for 1 min using Light Cycler96 SW1.1 (Roche).

Microarray analysis

WT and HIF-1 CKO BMDMs were infected with *M. tuberculosis* H37Rv (MOI = 0.5) for 12 h in DMEM excluding FBS. After extracellular bacilli had been removed from the macrophage culture medium, cells were cultured for 4 days in the presence of 500 U ml^{-1} IFN-γ. Total RNA (100 ng) extracted from macrophages using the PARIS™ Kit, according to the manufacturer's instructions was subjected to a microarray analysis. Complementary RNA labeled with either Cy3 or Cy5 was hybridized on the Gene Chip Mouse Gene 1.0 ST Array targeting 28 853 mouse genes (Affymetrix Inc., Santa Clara, CA, USA). The signature genes with fold changes >1.3 or <1/1.3 (<0.77) in HIF-1 CKO BMDMs than in WT BMDMs were subjected to further evaluations.

Intracellular growth of M. tuberculosis in macrophages

Mouse BMDMs (5×10^4 cells per well) seeded on a 96-well plate were infected (MOI = 0.5) with rMtb-luc for 12 h in DMEM excluding FBS, after which extracellular bacilli were removed from the macrophage culture medium. Macrophages infected with mycobacteria were cultured for 10 days in the absence or presence of 500 U ml^{-1} IFN-γ. An inhibitor of glycolytic enzymes,

100 mM oxamate or 0–11 mM pyruvate was added immediately after infection for 12 h. The intracellular bacilli in cell lysates were measured with a luciferase assay system (Promega, Madison, WI, USA) as follows. After an additional incubation of infected macrophages with 0.5% Triton X-100, cell lysates were mixed by well pipetting 30 times and 50 μl of the suspension was transferred into a 96-well black flat-bottomed plate (Sumitomo Bakelite, Tokyo, Japan). The same volume of luciferase assay reagent (Promega) was then added to the wells and luciferase activity was measured using a FilterMax F5 Multi-mode microplate reader (Molecular Devices, Osaka, Japan).

Measurement of extracellular lactate in macrophages

Mouse BMDMs (2×10^6 cells per well) seeded on six-well plates were infected with rMtb-luc (MOI = 0.5) for 12 h in DMEM excluding FBS, and extracellular bacilli were then removed from the macrophage culture medium. After 3 days in culture, the cell culture medium was collected. Lactate was measured with the L-lactate Assay Kit (Abcam, Cambridge, UK).

Measurement of intracellular pyruvate in macrophages

Mouse BMDMs (2×10^6 cells per well) seeded on six-well plates were infected with rMtb-luc (MOI = 0.5) for 12 h in DMEM excluding FBS, and extracellular bacilli were removed from the macrophage culture medium. After 0 and 6 days in culture, mouse BMDMs cells were collected with 5% mannitol and pyruvate was measured with the Pyruvate Assay Kit (BioVision Inc., Mountain View, CA, USA). RAW264.7 cells (1×10^5 cells per well) on 96-well plates were infected with rMtb-luc (MOI = 0.5) for 12 h and extracellular bacilli were removed from the macrophage culture medium. After 3 days in culture, pyruvate in RAW264.7 cells was measured with the Pyruvate Assay Kit (Abcam).

Measurement of intracellular glucose in macrophages

Mouse BMDMs (5×10^4 cells per well) and RAW264.7 cells (1×10^5 cells per well) on 96-well plate were infected with rMtb-luc (MOI = 0.5) for 12 h in DMEM excluding FBS, and extracellular bacilli were removed from the macrophage culture medium. After 3 days in culture, cells were washed by cold PBS to avoid contamination from glucose into medium. Glucose concentrations were measured with the Glucose-Glo Assay Kit (Promega).

Ingestion of [^{14}C]-pyruvate from macrophages

Mouse BMDMs (5×10^4 cells per well), seeded on a 96-well plate, were infected (MOI = 0 or 10) with BCG for 12 h in DMEM excluding FBS, and extracellular bacilli were removed from the macrophage culture medium. After culturing for 24 h in DMEM, 0.1 mM [^{14}C]-pyruvate was added to the macrophage culture medium. To assess the level of [^{14}C]-pyruvate in intracellular bacilli from infected macrophages, radioactivity was measured with a solid scintillation counter using glass fiber filter paper that trapped bacilli, but not the medium.

Effects of pyruvate and glucose on the growth of mycobacteria

rMtb-luc or rBCG-luc was cultured in 7H9 media containing 0% albumin and 0.085% NaCl with or without 0–10 mM pyruvate or glucose as the carbon source for 10 days. Bacterial growth was measured with the luciferase assay system.

Statistical analysis

Experiments were performed three times or more. All data are presented as means ± standard deviation (SD) of at least three independent biological replicates. Comparisons among groups were performed using the Student's *t*-test, a one-way analysis of variance (ANOVA) followed by Tukey's test or a two-way ANOVA followed by the Bonferroni test. Statistical analyses were performed with Graph Pad PRISM (Version 5.0). Differences were considered to be significant at a *P*-value < 0.05.

Results

Co-localization of HIF-1α and M. tuberculosis in mouse pulmonary granulomas

We stained tissue sections of mouse pulmonary granulomas with an anti-HIF-1α antibody to clarify whether HIF-1 is expressed in mouse TB granulomas. The expression of HIF-1α was not detected in uninfected mice (Fig. 1A-iii). In contrast, HIF-1α was strongly expressed at the center of granulomas (Fig. 1A-vii and Supplementary Figure 1-iii, vii) and the stained area largely coincided with the region stained with the acid-fast (Ziehl–Neelsen) stain (Fig. 1A-vi and Supplementary Figure 1-ii, vi). An antibody directed against MDP1 (Rv2986c), a major cellular protein of *M. tuberculosis* that is not secreted from bacilli (11), stained almost the same region as the anti-HIF-1α antibody (Fig. 1A-viii and Supplementary Figure 1-iv, viii). These results show the prominent co-localization of tubercle bacilli and HIF-1α in mouse TB granulomas.

According to Via *et al.*, the central region of human and not mouse TB granulomas becomes hypoxic (12). In the present study, we did not detect a hypoxic area in BALB/c mouse TB granulomas stained with pimonidazole, a hypoxic probe (Supplementary Figure 2, Supplementary Methods), which is consistent with previous findings (12). Peyssonnaux *et al.* (7) reported that HIF-1α is induced during the phagocytosis of several bacteria, including group A *Streptococcus*, *Staphylococcus aureus*, *Salmonella typhimurium*, and *P. aeruginosa*. Using BMDMs from mice, we investigated whether the expression of HIF-1α was induced by an infection with *M. tuberculosis* alone. Even under normoxic conditions, HIF-1α protein levels markedly increased 24 h after infection with two *M. tuberculosis* complex strains, *M. tuberculosis* H37Rv and *M. bovis* BCG (Fig. 1B). The increases caused by these infections were observed in naive and IFN-γ-activated BMDMs (Fig. 1B). HIF-1α expression was not detected in uninfected BMDMs in the absence or presence of IFN-γ. In contrast, HIF-2α expression was not detected in *M. Tuberculosis*-infected macrophages (Supplementary Figure 3A and B). Moreover, HIF-1β expression was not changed by infection with *M. tuberculosis* and IFN-γ. Thus, HIF-1α expression may be induced solely through the infection of mouse macrophages by *M. tuberculosis*.

HIF-1α protein levels are known to be largely regulated post-translationally under hypoxic conditions. However, we found that *Hif-1α* mRNA levels were 6-fold higher in BMDMs

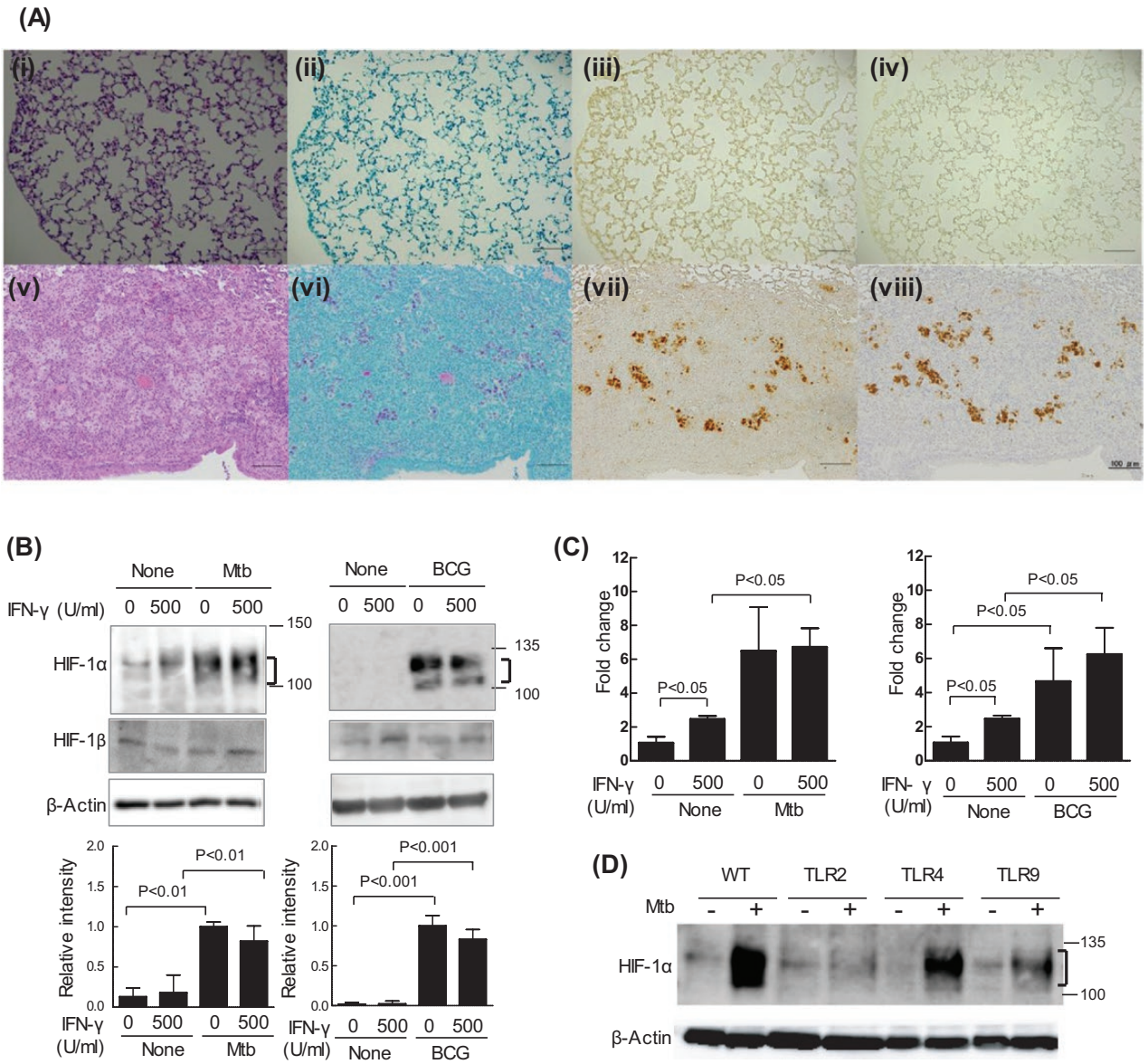

Fig. 1. Expression of HIF-1α in TB granulomas and macrophages. (A) The lungs of each of seven BALB/c mice 5 weeks after infection with or without *M. tuberculosis* Erdman were fixed in 10% formaldehyde. A normal mouse lung is shown in i–iv and mouse lung granuloma in v–viii. The mouse lung sections were stained with Hematoxylin-Eosin stain (i, v) or the Ziehl–Neelsen stain (ii, vi), and immune-stained with anti-HIF-1α IgG (iii, vii) and anti-MDP1 IgG (iv, viii). Scale bars: 100 μm (i–viii). (B and C) After infection with *M. tuberculosis* H37Rv (Mtb) or *M. bovis* BCG (BCG) for 12 h, BMDMs from WT mice were cultured for 24 h in the absence or presence of 500 U ml^{-1} IFN-γ. (B) Whole-cell lysates were fractionated on 7.5% polyacrylamide gels with sodium dodecyl sulfate-polyacrylamide gel electrophoresis (SDS-PAGE) and immunoblotted with an anti-HIF-1α antibody, anti-HIF-1β antibody or anti-β-actin antibody (as the loading control). Ratios of HIF-1α/β-actin are shown as relative intensities. Values are expressed as means ± SD from four independent biological replicates. (C) Amplified *Hif-1α* mRNA products were normalized to 18S rRNA. Values are expressed as the means ± SD from three independent biological replicates. (D) After infection with *M. tuberculosis* H37Rv for 12 h, BMDMs from WT mice or those lacking Toll-like receptor 2/4/9 (TLR2/4/9) were cultured for 24 h without 500 U ml^{-1} IFN-γ. Whole-cell lysates were fractionated on 7.5% polyacrylamide gels with SDS–PAGE and immunoblotted with an anti-HIF-1α antibody or anti-β-actin antibody (as the loading control). The significance of differences was assessed by a two-way analysis of variance (ANOVA) followed by the Bonferroni test.

infected with either mycobacterial strain than in uninfected BMDMs (Fig. 1C). Moreover, the accumulation of the HIF-1α protein depended on TLR2 and TLR9, and was independent of TLR4 (Fig. 1D). These results demonstrated that the expression and stabilization of the HIF-1α protein was induced solely through the infection of macrophages by mycobacteria via TLR2 and/or TLR9.

HIF-1α-deficient macrophages fail to suppress the intracellular growth of M. tuberculosis

To confirm the *in vivo* relevance of the HIF-1-mediated protection of macrophages against *M. tuberculosis*, we compared the survival kinetics of WT mice with those lacking HIF-1α in their myeloid cell lineage (HIF-1 CKO) after an intra-tracheal infection with *M. tuberculosis* H37Rv. Almost 50% of HIF-1 CKO

mice died within 45 days of infection, whereas all WT mice survived in the same duration (Fig. 2A). These results indicate that the expression of HIF-1 in macrophages plays a critical role in protecting the host against *M. tuberculosis in vivo*, which is consistent with previous findings reported by Braverman *et al.* (8).

To clarify whether HIF-1 influences the host-protective functions of macrophages, we analyzed the growth of *M. tuberculosis* in WT and HIF-1 CKO BMDMs *in vitro*. After an infection with recombinant *M. tuberculosis* expressing luciferase, we monitored bacterial viability by measuring light production caused by luciferase activity to oxidize the substrate luciferin. IFN-γ suppressed the intracellular growth of *M. tuberculosis* in WT BMDMs, but not that in HIF-1 CKO BMDMs. In IFN-γ-activated macrophages, the intracellular growth of *M. tuberculosis* was significantly greater in HIF-1 CKO BMDMs 4 and 10 days after infection than in WT BMDMs (Fig. 2B). In contrast, in naive macrophages without the IFN-γ stimulation, the intracellular growth of bacilli was greater in HIF-1 CKO BMDMs than in WT BMDMs, but not significantly. However, the increased ratio between 4 and 8 days after infection with *M. tuberculosis* in HIF-1 CKO BMDMs (shown by the slope in Fig. 2B) was significantly higher than that in WT BMDMs in the absence of IFN-γ (Fig. 2C). These results suggest that HIF-1 plays a suppressive role in the intracellular replication of *M. tuberculosis* in IFN-γ-activated and non-activated macrophages.

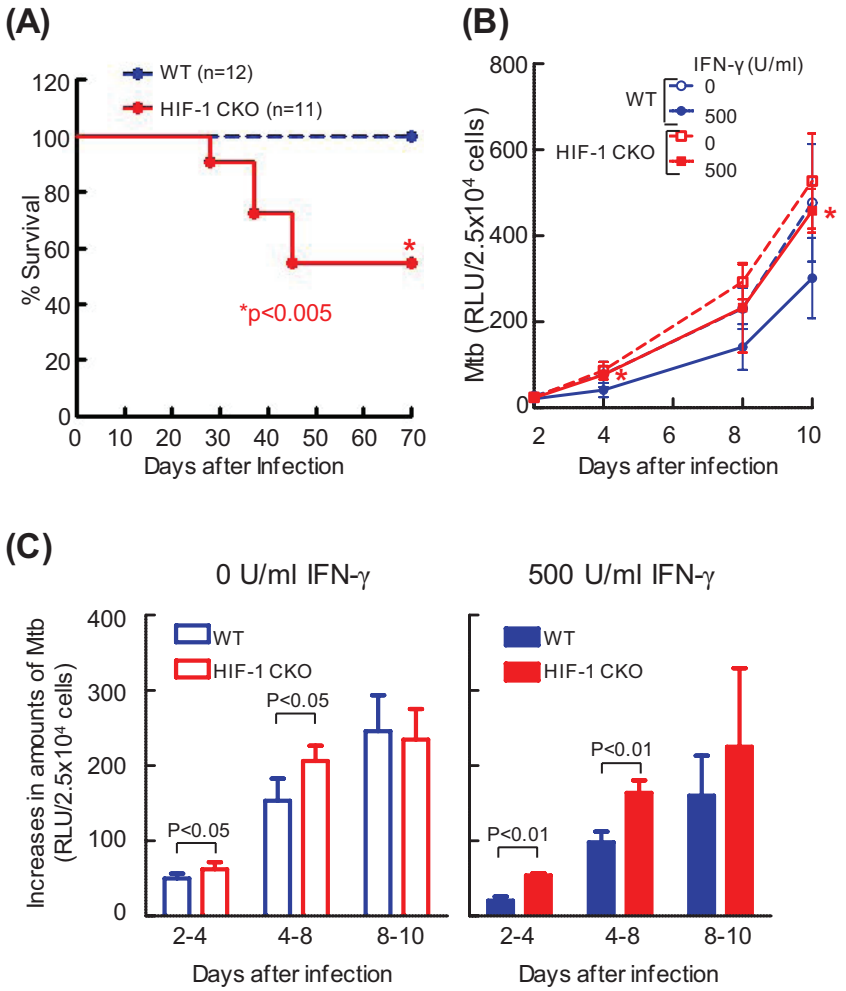

Fig. 2. HIF-1α-deficient macrophages failed to control *M. tuberculosis* growth. (A) WT mice or those lacking HIF-1α in their myeloid cell lineage (HIF-1 CKO) were infected with 2×10^6 CFU of the *M. tuberculosis* H37Rv strain via the intra-tracheal route. The graph shows the percentage survival of mice, with the total numbers indicated in parentheses. Data represent the means ± SD of 12 WT mice and 11 HIF-1 CKO mice. A Kaplan–Meier survival analysis showed that the probability of survival of HIF-1 CKO mice after *M. tuberculosis* infection was significantly lower than that of WT mice. The statistical significance of differences was assessed by the Log-rank test ($P = 0.0039$). (B) After BMDMs from WT or HIF-1 CKO mice were infected with kanamycin-resistant *M. tuberculosis* with luciferase (rMtb-luc) for 12 h, extracellular bacilli were removed from the macrophage culture medium. BMDMs were cultured for 10 days in DMEM with or without 500 U ml^{-1} IFN-γ. Intracellular *M. tuberculosis* growth was monitored by chemiluminescence (relative light units, RLU) with the luciferase assay system. Values are expressed as the means ± SD from four independent biological replicates. The statistical significance of differences was calculated by ANOVA followed by Student's *t*-test each infection day. *$P < 0.05$ was compared between WT and HIF-1 CKO in the presence of IFN-γ. (C) Increased amounts of intracellular *M. tuberculosis* from days 2 to 4, days 4 to 8 and days 8 to 10 after infection were expressed. Values are expressed as the means ± SD from four independent biological replicates. The statistical significance of differences was calculated by the Student's *t*-test.

LDH-A contributes to the HIF-1-mediated limitation of intracellular M. tuberculosis growth

To elucidate the host-protective mechanisms mediated by HIF-1, we examined the major anti-mycobacterial effectors induced by the IFN-γ stimulation because the effect of a HIF-1α deficiency is more pronounced in the presence of IFN-γ. The expression of 757 and 1190 genes was ≥1.3-fold stronger and ≤0.77-fold weaker, respectively, in HIF-1 CKO than in WT (Fig. 3A) (ArrayExpress accession: E-MTAB-7244). Moreover, the annotated genes in these genes, as Bioset1, were compared with Braverman's data (8) using an RNA seq analysis, as Bioset2. We found marked similarities in the gene expression profiles of Bioset1 and Bioset2 (Supplementary Figure 4).

The expression of 68 genes related to carbohydrate metabolism was weaker in HIF-1 CKO BMDMs than in WT BMDMs (HIF-1 CKO/WT ≤ 0.77). In Fig. 3(B), 34 genes (particularly HIF-1 CKO/WT ≤ 0.70) contained enzymes involved in glycolysis (red). In addition, the gene levels of two glycolytic enzymes, such as hexokinase 2 (NM_013820) and phosphoglycerate kinase 1 (NM_008828), were <0.77-fold those in HIF-1 CKO/WT. However, these genes were not shown in Fig. 3(B) because fold changes were >0.70. Moreover, the accumulation of lactate was observed in animal lungs infected with *M. tuberculosis* (13, 14), which implies that *M. tuberculosis* infection induces aerobic glycolysis in macrophages (namely, 'the production of ATP through glycolysis'). These results show that the expression of glycolysis-related genes, such as *Ldh-A*, was reduced by a HIF-1α deficiency (Fig. 3B). Thus, we confirmed the HIF-1-dependent transcriptional regulation of *Ldh-A* mRNA with real-time PCR. During an infection with *M. tuberculosis*, *Ldh-A* mRNA levels were markedly higher in WT BMDMs in the presence or absence of IFN-γ (Fig. 3C) than in HIF-1 CKO BMDMs. We also measured extracellular levels of lactate, which is metabolized from pyruvate by LDH-A. The results obtained revealed that lactate levels were higher in WT BMDMs than in HIF-1 CKO BMDMs (Fig. 3D).

In order to investigate whether LDH-A participates in the inhibition of the intracellular growth of *M. tuberculosis*, we examined the effects of LDH-A inhibitors. The LDH inhibitor, oxamate, significantly increased the growth of bacilli 4 days after infection in IFN-γ-stimulated and unstimulated BMDMs (Fig. 3E). Furthermore, the growth of *M. tuberculosis* was greater in *Ldh-A*-deficient RAW264.7 cells (LDH-A KO) than in WT cells (Fig. 3F). These results suggest that LDH-A contributes to the HIF-1-mediated restriction of intracellular *M. tuberculosis* replication in an IFN-γ-independent manner.

iNOS contributes to the IFN-γ-mediated limitation of intracellular M. tuberculosis growth

IFN-γ has been shown to induce the expression of iNOS and limits intracellular *M. tuberculosis* growth (15). In this study, a microarray analysis showed that *iNos* mRNA levels were 0.76-fold lower in HIF-1 CKO BMDMs than in WT BMDMs (by M.O.-O.; ArrayExpress accession: E-MTAB-7244). Thus, we compared *iNos* mRNA levels between WT and HIF-1 CKO BMDMs after an infection with *M. tuberculosis*. *iNos* mRNA levels were markedly increased by the combination of *M. tuberculosis* infection and the IFN-γ stimulation (Fig. 4A). *iNos* mRNA levels were lower in HIF-1 CKO BMDMs (by ~50%) than in WT BMDMs. Moreover, iNOS protein levels were ~60% lower in HIF-1 CKO BMDMs than in WT BMDMs (Fig. 4B). As expected, the growth of *M. tuberculosis* was greater in iNOS KO BMDMs than in WT BMDMs (Fig. 4C).

We revealed that the concentration of intracellular glucose increased in a HIF-1α-dependent manner (Supplementary Figure 5A). Moreover, a high concentration (4.5 g l^{-1}) of glucose alone enhanced the proliferation of *M. tuberculosis* in WT and HIF-1 CKO BMDMs (Supplementary Figure 5B). Similarly, the proliferation of *M. tuberculosis* was also enhanced, even in BMDMs derived from an iNOS KO mouse, when cells were cultured in medium containing a high concentration of glucose (Supplementary Figure 5C). These results indicate that the level of glucose and its metabolism strongly affect the limitation of intracellular *M. tuberculosis* growth. Interestingly, oxamate, the inhibitor of LDH, enhanced intracellular *M. tuberculosis* growth in iNOS KO BMDMs (Fig. 4D). These results suggest that LDH regulates the replication of bacilli in macrophages independently of iNOS; however, iNOS plays an important role in host defenses.

LDH inhibits the mycobacterial ingestion of pyruvate in macrophages

We showed that HIF-1 induced *Ldh-A* mRNA transcription during *M. tuberculosis* infection, resulting in a decrease in lactate concentrations (Fig. 3D). We next investigated the host-protective mechanism mediated by LDH. LDH converts pyruvate to lactate. Therefore, we assessed intracellular levels of pyruvate in WT and HIF-1 CKO BMDMs. The results revealed that intracellular pyruvate levels increased in HIF-1 CKO BMDMs immediately and 6 days after infection (Fig. 5A).

We examined whether the pathogen has the ability to take up host-derived pyruvate for its intracellular survival and replication. To test this hypothesis, we infected *in vitro*-cultured WT BMDMs with BCG and added [^{14}C]-labeled pyruvate to the cultured medium. We observed an absolute increase in [^{14}C] accumulation in the bacterial fraction (Fig. 5B). BCG remains in the phagosome and does not escape to the cytosol, similar to *M. tuberculosis* (16). Therefore, intracellular bacteria, even those in phagosomes, may take up exogenous pyruvate. In the present study, higher concentrations of pyruvate enhanced the intracellular growth of *M. tuberculosis* in macrophages with or without INF-γ (Fig. 5C). Moreover, the intracellular growth of *M. tuberculosis* was suppressed by excluding pyruvate in culture media (Supplementary Figure 6). It is defined that the intracellular growth of *M. tuberculosis* is higher in LDH-A KO cells than in WT cells in Fig. 3(F). Therefore, we examined whether pyruvate enhanced the mycobacteria growth in LDH-A KO cells. The concentration of intracellular pyruvate was higher in LDH-A KO cells than in WT cells (Fig. 5D). In contrast, the concentration of intracellular glucose was as same in LDH-A KO cells and WT cells. Furthermore, pyruvate was excluded in culture media, resulting in suppression of the intracellular growth of *M. tuberculosis* in WT cells, while a lack of pyruvate did not decrease in the intracellular growth of *M. tuberculosis* in LDH-A KO cells (Fig. 5E).

Most importantly, in the *in vitro* culture without macrophages, *M. tuberculosis* grew more rapidly in medium containing pyruvate as the sole carbon source than when glucose was added (Fig. 5F). This result demonstrated that

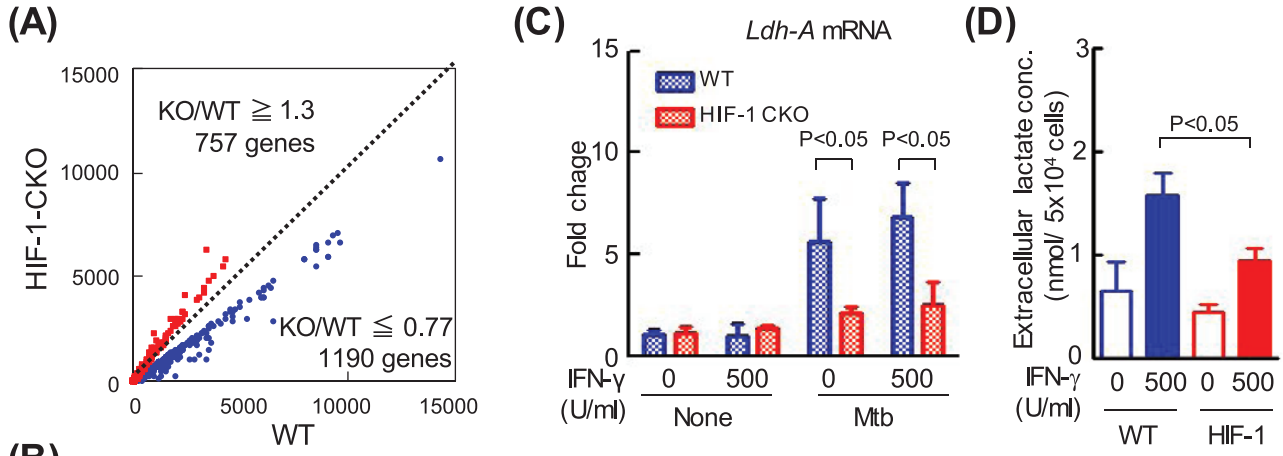

(B)

Gene Symbol	Gene Accession	CKO/WT
Gsta3	NM_001077353	0.70
Glul	BC015086	0.70
Slc37a4	NM_008063	0.70
P4ha1	NM_011030	0.70
Tpi1	NM_009415	0.70
Gstp2	NM_181796	0.70
Scd2	NM_009128	0.69
Gstm1	NM_010358	0.69
Grhpr	NM_080289	0.68
Napepld	NM_178728	0.67
Adssl1	NM_007421	0.66
Smox	NM_145533	0.66
Gstm2	NM_008183	0.65
Pygl	NM_133198	0.65
Ldha	NM_010699	0.64
Pfkl	NM_008826	0.63
Rhov	NM_145530	0.63
1100001H23Rik	BC019793	0.63
Pgm2	NM_028132	0.62
P4ha2	NM_001136076	0.60
Sgms2	NM_028943	0.60
Egln1	NM_053207	0.59
Gstp1	NM_013541	0.58
Mmp13	NM_008607	0.56
Pdpn	NM_010329	0.50
Pdk1	NM_172665	0.47
Phospho1	NM_153104	0.47
Aldoc	NM_009657	0.41
Uck2	NM_030724	0.41
Hyal1	NM_008317	0.38
Mmp12	NM_008605	0.32
Ak3l1	AB020239	0.21
Egln3	NM_028133	0.15
Mmp8	NM_008611	0.14

Fig. 3. HIF-1α controls the transcription of glycolytic enzymes in macrophages independent of IFN-γ. (A) After BMDMs from WT mice or those lacking HIF-1α in their myeloid cell lineage (HIF-1 CKO) were infected with *M. tuberculosis* H37Rv for 12 h, extracellular bacilli were removed from the macrophage culture medium. BMDMs were cultured for 4 days with 500 U ml^{-1} IFN-γ. Gene expression in macrophages was analyzed using microarrays, and is shown on scatterplots. The number of genes with expression levels that were higher in WT macrophages than in HIF-1 CKO (CKO/WT ≤ 0.77) was 1190, while that of those with lower expression levels (CKO/WT ≥ 1.30) was 757. (B) In the microarray analysis, metabolite enzymes with decreased expression levels in HIF-1 CKO BMDMs (KO/WT ≤ 0.70) are listed (34 genes); glycolysis enzymes are shown in red (11 genes). (C) After WT or HIF-1 CKO BMDMs were infected with *M. tuberculosis* H37Rv (Mtb) for 12 h, extracellular bacilli were removed from the macrophage culture medium. BMDMs were cultured for 24 h with or without 500 U ml^{-1} IFN-γ. Amplified *Ldh-A* mRNA products were normalized to 18S rRNA. Values are expressed as the means ± SD from three independent biological replicates. (D) After WT or HIF-1 CKO BMDMs had been infected with Mtb, extracellular bacilli were removed from the macrophage culture medium. BMDMs were cultured for 3 days with or without 500 U ml^{-1} IFN-γ. Extracellular levels of lactate in WT or HIF-1 CKO BMDMs were measured using a photometer. Values were expressed as the means ± SE from 4–6 independent biological replicates. (E) After WT BMDMs had been infected with the kanamycin-resistant *M. tuberculosis* with luciferase (rMtb-luc) strain for 12 h, extracellular bacilli were removed from the macrophage culture medium. BMDMs were cultured for 3 days in the presence or absence of 100 mM oxamate (Oxa), an LDH inhibitor. Intracellular *M. tuberculosis* growth was monitored by chemiluminescence (relative light units, RLU) with the luciferase assay system. Data represent the means ± SD from four independent biological replicates. (F) RAW264.7 macrophages (WT) and LDH-A KO, in which *Ldh-A* was deleted using the CRISPR/Cas9 system, were infected with rMtb-luc for 12 h, and macrophages were then cultured for 4 days. Intracellular *M. tuberculosis* growth was monitored by chemiluminescence. Data represent the means ± SD from 3–5 independent biological replicates. The statistical significance of differences was calculated by a two-way ANOVA followed by the Bonferroni test (C–E) or Student's *t*-test (F).

pyruvate is the preferred carbon source of *M. tuberculosis*. Similarly, the growth of BCG was enhanced in a pyruvate-dependent manner (Fig. 5G and H). These results indicate that intracellular bacteria have the ability to ingest pyruvate from host cells and utilize it as a source of energy for intracellular survival and replication.

Collectively, the present results indicate that the HIF-1-dependent up-regulation of LDH enhances the conversion of

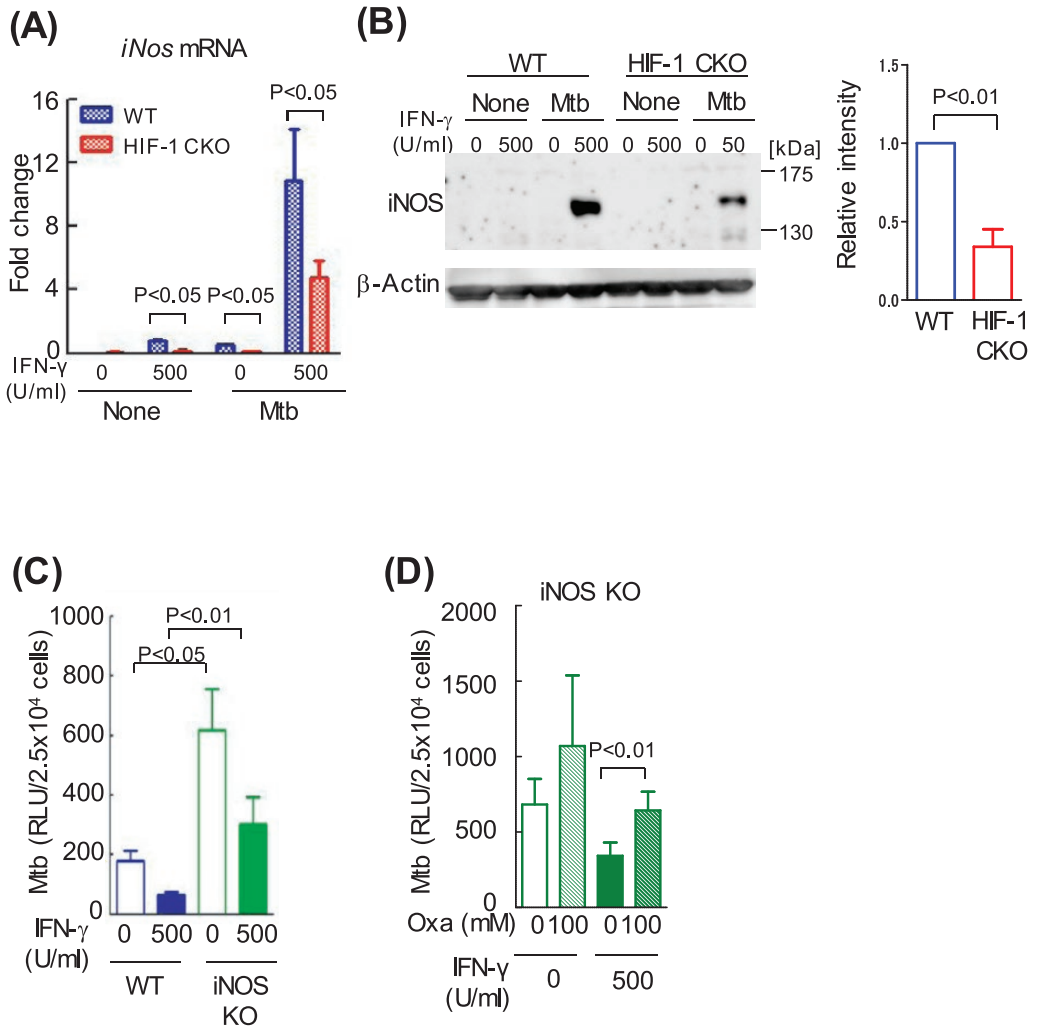

Fig. 4. HIF-1α-dependent up-regulation of iNOS after IFN-γ activation. (A and B) After BMDMs from WT mice or those lacking HIF-1α in their myeloid cell lineage (HIF-1 CKO) were infected with *M. tuberculosis* H37Rv (Mtb) for 12 h, extracellular bacilli were removed from the macrophage culture medium. BMDMs were cultured for 24 h with or without 500 U ml^{-1} IFN-γ. Amplified iNos mRNA products were normalized to 18S rRNA. Data represent the means ± SD from four independent biological replicates (A). Whole-cell lysates were fractionated on 7.5% polyacrylamide gels with SDS–PAGE and immunoblotted with an anti-iNOS antibody or anti-β-actin antibody (as the loading control). The ratio of iNOS/β-actin with 500 U ml^{-1} IFN-γ and *M. tuberculosis* was shown (B). Data represent the means ± SD from three independent biological replicates. (C and D) After BMDMs from WT mice or those lacking iNOS were infected with the kanamycin-resistant *M. tuberculosis* with luciferase (rMtb-luc) strain for 12 h, extracellular bacilli were removed from the macrophage culture medium. BMDMs were cultured for 4 days with or without 500 U ml^{-1} IFN-γ (C), or in the absence or presence of 100 mM oxamate (Oxa), an LDH inhibitor (D). Intracellular *M. tuberculosis* growth was monitored by chemiluminescence (relative light units, RLU) with the luciferase assay system. Data represent the means ± SD from three independent biological replicates. The statistical significance of differences was assessed by a two-way ANOVA followed by the Bonferroni test (A), (C) and (D), or the Student's *t*-test (B).

pyruvate to lactate, which is a fundamental mechanism for restricting the intracellular growth of *M. tuberculosis*.

Discussion

In the present study, we evaluated the host-protective functions of HIF-1 against TB. We detected HIF-1α expression in pulmonary TB granulomas in mice. The location of HIF-1α was similar to acid-fast stained bacilli and was more consistent with that of MDP1 (Irep-28), a major cellular protein of mycobacteria (11) (Fig. 1A). Previous studies reported that dormant *M. tuberculosis* loses acid-fastness *in vivo* by stunting cell wall synthesis (17, 18). In contrast, MDP1 is up-regulated under growth-retarded states, such as iron-limited conditions (19), dormancy and persistent infection in humans (20). Therefore, the co-localization of HIF-1α and MDP1 rather than with acid-fast staining may reflect the bacteriostatic efficacy of HIF-1α, as demonstrated in the present study. TB granulomas in guinea pigs, rabbits and non-human primates are hypoxic, whereas murine TB granulomas were recently shown to have a slightly lower pO_2 than those of other animals (12). We also found that the expression and stabilization of HIF-1α occurred when *in vitro*-cultured BMDMs were infected with *M. tuberculosis* or BCG only, even under normoxic conditions (Fig. 1B and C), as was also reported for infections with other pathogenic bacteria (7).

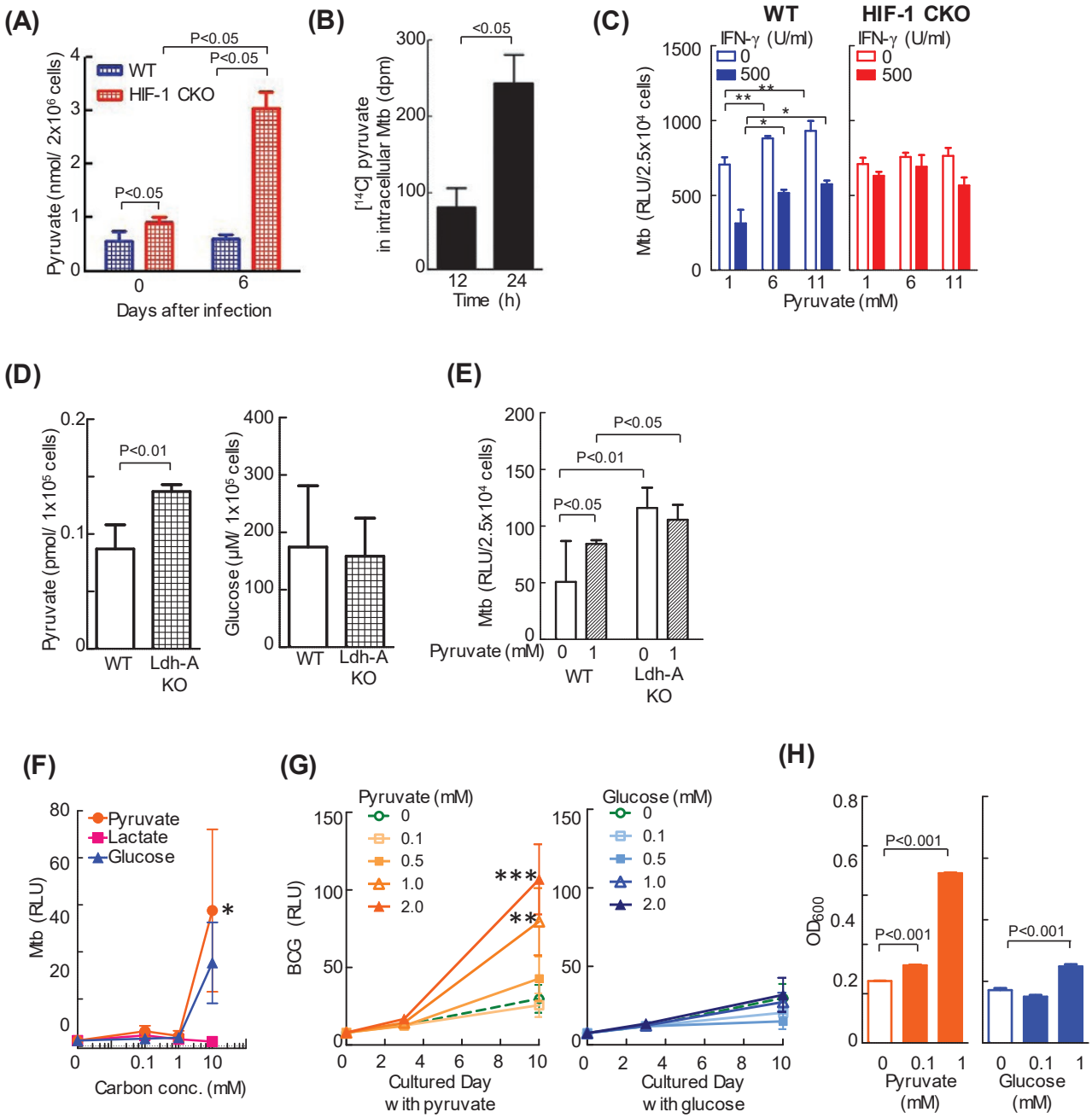

Fig. 5. Pyruvate up-regulates the replication of intracellular mycobacteria. (A) After BMDMs from WT mice or those lacking HIF-1α in their myeloid cell lineage (HIF-1 CKO) were infected with the kanamycin-resistant *M. tuberculosis* with luciferase (rMtb-luc) strain for 12 h, extracellular bacilli were removed from the macrophage culture medium. BMDMs were cultured for 0 or 6 days without 500 U ml^{-1} IFN-γ. The level of intracellular pyruvate was measured with a photometer. Data represent the means ± SD from three independent biological replicates. The statistical significance of differences was calculated by two-way ANOVA followed by the Bonferroni test. (B) After WT BMDMs were infected with the *M. bovis* BCG (BCG) strain for 24 h, extracellular bacilli were removed from the macrophage culture medium. BMDMs were cultured for 12 or 24 h with 0.1 mM [^{14}C]-pyruvate in medium containing 1 mM unlabeled pyruvate. The intracellular level of [^{14}C]-pyruvate was measured with a solid scintillation counter. Data represent the means ± SD of four independent biological replicates. The statistical significance of differences was calculated by Student's *t*-test. (C) After WT and HIF-1 CKO BMDMs were infected with rMtb-luc for 12 h, extracellular bacilli were removed from the macrophage culture medium. BMDMs were cultured for 6 days in medium containing 1, 6 or 11 mM pyruvate. The growth of intracellular bacteria was measured by chemiluminescence (relative light units, RLU) with the luciferase assay system. Data represent the mean ± SD from four independent biological replicates. The statistical significance of differences was calculated by one-way ANOVA in each group (0 or 500 U ml^{-1} IFN-γ). (D and E) RAW264.7 macrophages (WT) and LDH-A KO, in which *Ldh-A* was deleted using the CRISPR/Cas9 system, were infected with rMtb-luc strain for 24 h, extracellular bacilli were removed from the macrophage culture medium. After culture of RAW264.7 cells for 3 days, the pyruvate and glucose concentration were measured (D). After infection with *M. tuberculosis*, RAW264.7 cells were cultured for 3 days in medium with or without 1 mM pyruvate. Data represent the mean ± SD from four independent biological replicates. The statistical significance of differences was calculated by Student's *t*-test (D) and two-way ANOVA followed by the Bonferroni test (E). (F) rMtb-luc was incubated for 17 days in 7H9 medium containing pyruvate, lactate or glucose (0–10 mM) as the sole carbon source. The growth of bacteria

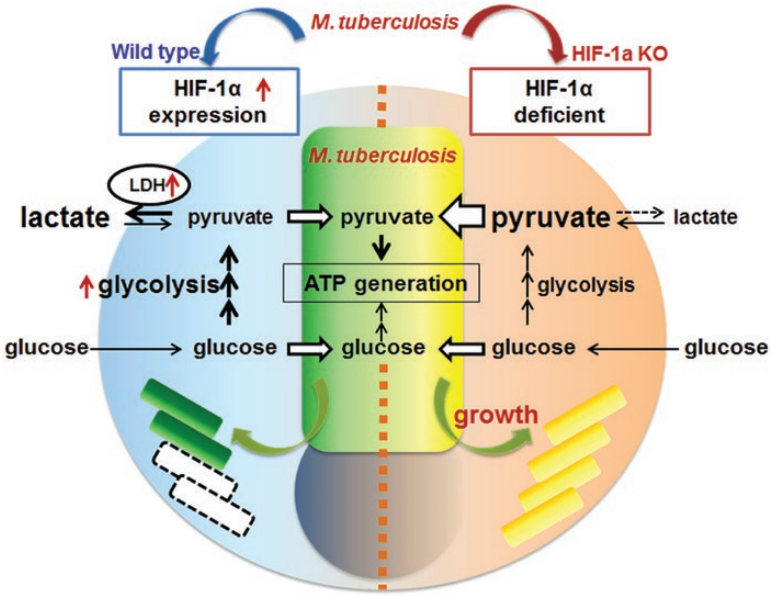

Fig. 6. HIF-1α-dependent glycolysis metabolism is a basic bacteriostatic mechanism to control *M. tuberculosis* replication in macrophages. *Mycobacterium tuberculosis* preferentially utilizes a host's pyruvate for its intracellular proliferation. Therefore, to protect the host, macrophages reduce the cellular concentration of pyruvate. HIF-1α, which is up-regulated during bacterial infection, enhances glucose metabolism in glycolysis. Consequently, the level of cellular pyruvate is reduced through its conversion to lactate by LDH, one of the proteins up-regulated by HIF-1. Therefore, HIF-1α-dependent glycolysis metabolism must be a fundamental host defense mechanism against intracellular bacteria, independent of IFN-γ.

Previous studies demonstrated that even under normoxic conditions, the HIF-1α protein is up-regulated via the stimulation of TLR4 by lipopolysaccharide (LPS) (21, 22), and via infections with Gram-positive or -negative bacteria, such as group A *Streptococcus* (7) and *Enterobacteriaceae* (23). In contrast, we found that TLR2 mostly and TLR9 slightly mediated increases in HIF-1α levels upon mycobacterial infections, whereas TLR4 did not (Fig. 1D). Mycobacteria secrete absolute amounts of TLR2 ligands, such as 19-kD lipoprotein, lipoarabinomannan and mannosyl-phosphatidylinositol, and strongly stimulate TLR2 residing on the plasma membrane (24). Moreover, mycobacterial genomic DNA, which is a TLR9 ligand, may be released after bacterial death and moderately stimulates TLR9 distributed on the phagosomal membrane (25). In addition, Sher's group reported that TLR2 and TLR9, but not TLR4 knockout mice were susceptible to *M. tuberculosis* infection, showing the importance of TLR2 and TLR9 in host protection (25). HIF-1-dependent host defense mechanisms against intracellular mycobacteria may be shared with TLR2- and TLR9-dependent mechanisms. A recent study demonstrated that HIF-1α was primarily important for the control of *M. tuberculosis* through the production of iNOS in IFN-γ-activated macrophages (8). IFN-γ is known to play central protective roles against intracellular pathogens. Moreover, *Irgm* mRNA (LRG-47), which is induced by IFN-γ (15), was shown to be involved in autophagosome formation, and the generation of reactive nitrogen intermediates, which are mediated by iNOS (26). Consistent with the findings reported by Braverman *et al.* (8), the present results show that iNOS is a key factor in HIF-1α$^{-/-}$ macrophages (Fig. 4). In contrast, HIF-1-dependent host defenses are independent of IFN-γ-dependent IRGM. The reason for this is that intracellular *M. tuberculosis* replication was not restricted even though IFN-γ increased *Irgm* mRNA levels in HIF-1α$^{-/-}$ macrophages (Supplementary Figure 7). Thus, HIF-1-dependent host defenses may be independent of IRGM. Interestingly, HIF-1α contributed to host protection in the absence of IFN-γ (Fig. 2C), and the attenuation of glucose metabolism by the LDH inhibitor strongly affected the limitation of intracellular *M. tuberculosis* growth in WT and iNOS$^{-/-}$ macrophages (Figs 3E, 3F and 4D). The presence of HIF-1-binding motifs in the LDH promoter region has already been reported (27). Lactate is transported out of the cell because increases in LDH expression induce cellular acidosis, which triggers apoptosis. Under normoxic conditions, cells generally metabolize glucose to CO_2 and water in an oxygen-dependent and highly

was measured by chemiluminescence (RLU). Data represent the mean ± SD from four independent biological replicates. The statistical significance of differences was calculated by one-way ANOVA in each carbon dose. *$P < 0.05$ versus 10 mM lactate. (G) rBCG-luc was incubated for 10 days in 7H9 medium containing either pyruvate or glucose (0–2.0 mM) as the sole carbon source. The growth of bacilli was monitored by chemiluminescence (RLU). Data represent the means ± SD from three or four independent biological replicates. The statistical significance of differences was calculated by one-way ANOVA in each cultured day. **$P < 0.01$, and ***$P < 0.001$ versus 0 mM pyruvate. (H) rBCG-luc was incubated for 10 days in 7H9 medium containing either pyruvate or glucose (0.1 or 1.0 mM) as the sole carbon source. The amounts of BCG were measured by a photometer at 600 nm. Data represent the means ± SD from five independent biological replicates. The statistical significance of differences was calculated by one-way ANOVA.

energy-efficient manner with the production of ATP via oxidative phosphorylation in mitochondria. This metabolism mainly involves glucose conversion to pyruvate followed by pyruvate catabolism through the tricarboxylic acid (TCA) cycle. In contrast, macrophage activity is enhanced by the metabolism of glucose via the LDH conversion of pyruvate to lactate. Shi *et al.* (28) confirmed an increase in the expression of key glycolytic enzymes together with increases in HIF-1α mRNA and protein levels in macrophages and T cells in granulomatous lesions. Cells mainly adapt to low oxygen tension by switching from an aerobic to anaerobic glycolytic pathway for ATP production. However, as monocytes differentiate into macrophages, they shift to glycolytic metabolism and thereby respond rapidly to low oxygen exposure in inflammation sites (29). Accordingly, the expression of glucose transporter 1 and glycolytic enzymes, including LDH, may be higher in macrophages than in monocytes, while energy production through the TCA cycle was lower in macrophages than in monocytes. Interestingly, the accumulation of TCA cycle intermediates, such as succinate, was similar in HIF-1α$^{-/-}$ and WT macrophages (Supplementary Figure 8). This result implies a shift from an aerobic TCA cycle to an anaerobic glycolytic pathway in *M. tuberculosis*-infected HIF-1α$^{-/-}$ macrophages. The present results showed that glycolytic metabolism was significantly enhanced in macrophages following *M. tuberculosis* infection, as implied by the increased activities of glycolytic enzymes (Fig. 3B). On the other hand, HIF-1α$^{-/-}$ macrophages failed to adapt to glycolytic metabolism, resulting in low levels of lactate and high levels of pyruvate in HIF-1α$^{-/-}$ macrophages (Figs 3D and 5A).

Similar to many bacteria, glycolysis and the TCA cycle occur in *M. tuberculosis*. The first committed step in glucose metabolism is the phosphorylation of glucose by glucokinase to produce glucose-6-phosphate in glycolysis. The genome contains *ppgK* (Rv2702) and *glkA* (Rv0650), which encode a polyphosphate glucokinase (30). PPGK is sufficient for *M. tuberculosis* to utilize glucose as a carbon source for *in vitro* growth, but is insufficient under *in vivo* conditions, as shown by the failure of the *ppgK* mutant to replicate and survive in mice. Therefore, glucose may be a substrate for growth or metabolism. However, *M. tuberculosis* preferentially uses a host's lipids as a carbon source for growth and persistence during infection (31). Mycobacterial growth in medium containing glycerol was found to be greater than that with glucose as the carbon source (32). Intracellular bacteria uptake glycerol and utilize it for ATP production through its conversion to pyruvate via glyceraldehyde-3-phosphate. The TCA cycle is essential in cell metabolism and requires pyruvate as the first substrate. Tian *et al.* (33) showed that *M. tuberculosis* operated the TCA cycle during infection in macrophages. Thus, pyruvate may be a key substrate for energy production in intracellular *M. tuberculosis*.

Pyruvate is one of the key intersections in metabolic pathways and may supply energy to bacteria and eukaryotic cells under aerobic and anaerobic conditions. Therefore, it is reasonable for phagocytic cells to employ a mechanism to limit the level of pyruvate, which supports the intracellular growth of pathogens. In contrast, *Escherichia coli* and *Salmonella enteritidis* prefer glucose to pyruvate for growth (Supplementary Figure 9). Although the infection-induced stabilization and up-regulation of the HIF-1α protein is conserved against infections by various bacterial pathogens in macrophages, the immediate metabolic adaptation to glycolysis mediated by HIF-1 needs to be the basic mechanism underlying host defenses in mycobacteria-infected macrophages.

In conclusion, we herein demonstrated that decreases in intracellular pyruvate concentrations due to increases in LDH expression regulated by HIF-1α restricted *M. tuberculosis* replication because pyruvate is a feasible carbon source for intracellular *M. tuberculosis* Fig. 6.

Funding

This work was supported by grants from the Ministry of Education, Culture, Sports, Science and Technology (21790130, 24790421), AMED Grant, Emerging & Re-emerging infection, 4582, the Japan Health Sciences Foundation, JSPS KAKENHI Grant (275057, 16H05187), and the United States–Japan Cooperative Medical Science Program against Tuberculosis and Leprosy, and Japan Foundation for Applied Enzymology.

Acknowledgements

We thank Katsura Mizushima (Department of Molecular Gastroenterology and Hepatology, Kyoto Prefectural University of Medicine, Kyoto, Japan) for microarray analysis. We are grateful for the heartfelt support and encouragement from Ms. Sara Matsumoto. M.O.-O., N.G., H.S., M.Y., Y.O., T.Y., T.S., Y.T., D.O. and S.M. performed experiments; M.O.-O., N.G. and S.M. designed the work and wrote the manuscript; K.T., K.M. and K.K. provided advice.

Conflicts of interest statement: the authors declared no conflicts of interest.

References

1 Flynn, J. L. and Chan, J. 2001. Immunology of tuberculosis. *Annu. Rev. Immunol.* 19:93.
2 Wang, G. L., Jiang, B. H., Rue, E. A. and Semenza, G. L. 1995. Hypoxia-inducible factor 1 is a basic-helix-loop-helix-PAS heterodimer regulated by cellular O_2 tension. *Proc. Natl Acad. Sci. USA* 92:5510.
3 Wang, G. L. and Semenza, G. L. 1995. Purification and characterization of hypoxia-inducible factor 1. *J. Biol. Chem.* 270:1230.
4 Ivan, M., Kondo, K., Yang, H. *et al.* 2001. HIFalpha targeted for VHL-mediated destruction by proline hydroxylation: implications for O_2 sensing. *Science* 292:464.
5 Jaakkola, P., Mole, D. R., Tian, Y. M. *et al.* 2001. Targeting of HIF-alpha to the von Hippel-Lindau ubiquitylation complex by O_2-regulated prolyl hydroxylation. *Science* 292:468.
6 Schaible, B., McClean, S., Selfridge, A. *et al.* 2013. Hypoxia modulates infection of epithelial cells by *Pseudomonas aeruginosa*. *PLoS One* 8:e56491.
7 Peyssonnaux, C., Datta, V., Cramer, T. *et al.* 2005. HIF-1alpha expression regulates the bactericidal capacity of phagocytes. *J. Clin. Invest.* 115:1806.
8 Braverman, J., Sogi, K. M., Benjamin, D., Nomura, D. K. and Stanley, S. A. 2016. HIF-1α is an essential mediator of IFN-γ-dependent immunity to *Mycobacterium tuberculosis*. *J. Immunol.* 197:1287.
9 Katsube, T., Matsumoto, S., Takatsuka, M. *et al.* 2007. Control of cell wall assembly by a histone-like protein in Mycobacteria. *J. Bacteriol.* 189:8241.
10 Matsumoto, S., Tamaki, M., Yukitake, H. *et al.* 1996. A stable *Escherichia coli*-mycobacteria shuttle vector 'pSO246' in *Mycobacterium bovis* BCG. *FEMS Microbiol. Lett.* 135:237.
11 Aoki, K., Matsumoto, S., Hirayama, Y. *et al.* 2004. Extracellular mycobacterial DNA-binding protein 1 participates in

mycobacterium-lung epithelial cell interaction through hyaluronic acid. *J. Biol. Chem.* 279:39798.
12 Via, L. E., Lin, P. L., Ray, S. M. *et al.* 2008. Tuberculous granulomas are hypoxic in guinea pigs, rabbits, and nonhuman primates. *Infect. Immun.* 76:2333.
13 Somashekar, B. S., Amin, A. G., Rithner, C. D. *et al.* 2011. Metabolic profiling of lung granuloma in *Mycobacterium tuberculosis* infected guinea pigs: *ex vivo* 1H magic angle spinning NMR studies. *J. Proteome Res.* 10:4186.
14 Shin, J. H., Yang, J. Y., Jeon, B. Y. *et al.* 2011. (1)H NMR-based metabolomic profiling in mice infected with *Mycobacterium tuberculosis*. *J. Proteome Res.* 10:2238.
15 MacMicking, J. D., Taylor, G. A. and McKinney, J. D. 2003. Immune control of tuberculosis by IFN-gamma-inducible LRG-47. *Science* 302:654.
16 Simeone, R., Bobard, A., Lippmann, J. *et al.* 2012. Phagosomal rupture by *Mycobacterium tuberculosis* results in toxicity and host cell death. *PLoS Pathog.* 8:e1002507.
17 Wayne, L. G. and Lin, K. Y. 1982. Glyoxylate metabolism and adaptation of *Mycobacterium tuberculosis* to survival under anaerobic conditions. *Infect. Immun.* 37:1042.
18 Seiler, P., Ulrichs, T., Bandermann, S. *et al.* 2003. Cell-wall alterations as an attribute of *Mycobacterium tuberculosis* in latent infection. *J. Infect. Dis.* 188:1326.
19 Yeruva, V. C., Duggirala, S., Lakshmi, V., Kolarich, D., Altmann, F. and Sritharan, M. 2006. Identification and characterization of a major cell wall-associated iron-regulated envelope protein (Irep-28) in *Mycobacterium tuberculosis*. *Clin. Vaccine Immunol.* 13:1137.
20 Osada-Oka, M., Tateishi, Y., Hirayama, Y. *et al.* 2013. Antigen 85A and mycobacterial DNA-binding protein 1 are targets of immunoglobulin G in individuals with past tuberculosis. *Microbiol. Immunol.* 57:30.
21 Blouin, C. C., Pagé, E. L., Soucy, G. M. and Richard, D. E. 2004. Hypoxic gene activation by lipopolysaccharide in macrophages: implication of hypoxia-inducible factor 1alpha. *Blood* 103:1124.
22 Frede, S., Stockmann, C., Freitag, P. and Fandrey, J. 2006. Bacterial lipopolysaccharide induces HIF-1 activation in human monocytes via p44/42 MAPK and NF-kappaB. *Biochem. J.* 396:517.
23 Hartmann, H., Eltzschig, H. K., Wurz, H. *et al.* 2008. Hypoxia-independent activation of HIF-1 by *Enterobacteriaceae* and their siderophores. *Gastroenterology* 134:756.
24 Thoma-Uszynski, S., Stenger, S., Takeuchi, O. *et al.* 2001. Induction of direct antimicrobial activity through mammalian Toll-like receptors. *Science* 291:1544.
25 Bafica, A., Scanga, C. A., Feng, C. G., Leifer, C., Cheever, A. and Sher, A. 2005. TLR9 regulates Th1 responses and cooperates with TLR2 in mediating optimal resistance to *Mycobacterium tuberculosis*. *J. Exp. Med.* 202:1715.
26 Chan, J., Xing, Y., Magliozzo, R. S. and Bloom, B. R. 1992. Killing of virulent *Mycobacterium tuberculosis* by reactive nitrogen intermediates produced by activated murine macrophages. *J. Exp. Med.* 175:1111.
27 Ebert, B. L. and Bunn, H. F. 1998. Regulation of transcription by hypoxia requires a multiprotein complex that includes hypoxia-inducible factor 1, an adjacent transcription factor, and p300/CREB binding protein. *Mol. Cell. Biol.* 18:4089.
28 Shi, L., Salamon, H., Eugenin, E. A., Pine, R., Cooper, A. and Gennaro, M. L. 2015. Infection with *Mycobacterium tuberculosis* induces the Warburg effect in mouse lungs. *Sci. Rep.* 5:18176.
29 Roiniotis, J., Dinh, H., Masendycz, P. *et al.* 2009. Hypoxia prolongs monocyte/macrophage survival and enhanced glycolysis is associated with their maturation under aerobic conditions. *J. Immunol.* 182:7974.
30 Marrero, J., Trujillo, C., Rhee, K. Y. and Ehrt, S. 2013. Glucose phosphorylation is required for *Mycobacterium tuberculosis* persistence in mice. *PLoS Pathog.* 9:e1003116.
31 Badalà, F., Nouri-mahdavi, K. and Raoof, D. A. 2014. Functional polarization of tumour-associated macrophages by tumour-derived lactic acid. *Nature* 513:559.
32 Hasan, M. R., Rahman, M., Jaques, S., Purwantini, E. and Daniels, L. 2010. Glucose 6-phosphate accumulation in mycobacteria: implications for a novel F420-dependent anti-oxidant defense system. *J. Biol. Chem.* 285:19135.
33 Tian, J., Bryk, R., Itoh, M., Suematsu, M. and Nathan, C. 2005. Variant tricarboxylic acid cycle in *Mycobacterium tuberculosis*: identification of alpha-ketoglutarate decarboxylase. *Proc. Natl Acad. Sci. USA* 102:10670.